Detection and Analysis of Time-Dependent Earthquake and Volcanic Processes using Space Geodesy

Paul Segall
Department of Geophysics
Stanford University
Stanford, CA 94305
segall@stanford.edu

Ken Hurst
JPL
Pasadena, CA
hurst@cobra.jpl.nasa.gov

Jeff McGuire
Dept of Geology and Geophysics
Woods Hole Oceanographic Institution
Woods Hole MA, 02543
jmcguire@whoi.edu

February 8, 2002

Contents

1 Abstract

With the development of large permanent GPS arrays, including SCIGN in southern California and GEONET in Japan, as well as InSAR displacement mapping, we now have deformation measurements that are dense in both space and time. These data permit the study of transient earthquake and volcanic processes that were not previously possible. Postseismic relaxation, as well as pre- and co-eruptive processes are all associated with time-varying strain. Recently, an entirely new class of aseismic processes, including silent earthquakes have been discovered. Within the past several years, silent earthquakes have been detected in southwest Japan, the Cascade subduction zone, and beneath Kilauea volcano. Detection, characterization, and analysis of these largely aseismic processes requires new inversion methods.

Recent improvements in the Network Inversion Filter coinciding with increased availability and precision of space geodetic measurements encourage us to propose an ambitious plan to study the spatial and temporal characteristics of transient deformation processes. Specifically we propose four principal tasks: 1) Completion of the Network Inversion Filter, including non-negativity constraints and automated determination of spatial and temporal smoothing parameters. 2) Development of a Network Strain Filter (NSF) for monitoring large regions and detecting deformation transients. The NSF does not require a specific source parameterization and is thus better suited to detecting subtle strain transients in large volumes of data. 3) Application of the NSF and NIF to the SCIGN GPS data. This effort will represent a concerted effort to detect and characterize aseismic transient motion in these data. It also represents our first attempt at extracting time variable deformation in a region with multiple active faults. 4) Application of the Network Inversion Filter to an ongoing aseismic deformation episode in the Tokai Gap, Japan. Beginning in mid 2000 GPS stations in the Tokai area began to record anomalous and accelerating crustal deformation. The anomalous motions are coherent at numerous stations and recorded by independent leveling data. This data is the best yet recorded of a large transient downdip of a locked megathrust. While similar events may have occurred in the past few decades we can not preclude the possibility that the aseismic slip will be followed by seismic rupture.

The proposed work will help to address the question: "What are the motions of the Earth and the Earth's interior and what information can be inferred about the Earth's internal processes?" Specifically, the work will support the study of extreme events including earthquakes and volcanic eruptions.

2 Technical Plan

2.1 Background

In the past decade there has been a tremendous increase in the number and density of geodetic networks for the study of crustal deformation. Large-scale permanent GPS arrays have been developed in Southern California (SCIGN) [*Bock et al.* 1997; *Hudnut et al.* 2001], in Japan (GEONET) [*Miyazaki et al.,* 1997; *Mazzotti et al.,* 2000], the Basin and Range (BARGEN) [*Wernicke et al.,* 2000], the Pacific Northwest (PANGA) [*Miller et al.,* 2001], the the San Francisco Bay region (BARD) [e.g., *Murray and Segall,* 2001], and elsewhere. Plans for the Plate Boundary Observatory (PBO) call for 1,000 permanent GPS sites in addition to 175 borehole strainmeters. These GPS networks yield daily estimates of site positions with a precision of 1 to 2 millimeters in the horizontal and 3-4 mm in the vertical over regional distances [*Hurst,* 2001], and are for the first time providing deformation data that is dense in both space and time.

The last decade has also witnessed an explosive growth in the use of interferometric SAR (InSAR) for the measurement of crustal deformation [e.g., *Burgmann et al.,* 2000]. INSAR maps of ground deformation have now been obtained for earthquakes [e.g., *Massonnet et al.,* 1993; *Fialko et al.*, 2001], post-seismic deformation [e.g., *Peltzer et al.,* 1996] and volcanic deformation [*Wicks et al.,* 2000; *Amelung et al.,* 2000]. Recent results have been obtained showing the interseismic pattern of deformation across the San Andreas and North Anatolian Faults [*Wright et al.,* 2001]. While existing spacecraft provide only limited temporal resolution, the potential for a repeat pass interferometry mission (such as ECHO), promise even greater spatial and temporal data densities.

Until rather recently much of the geophysical community's research effort has focused on obtaining accurate interseismic velocities from GPS networks, and analyzing coseismic displacement fields obtained by both GPS and InSAR. More recently, transient deformation events have been discovered that point to entirely new processes, such as silent earthquakes. Because these events are invisible to seismic instrumentation, silent deformation events are an important and challenging target for space geodesy. Silent earthquakes have now been discovered by permanent GPS networks in southwest Japan [*Hirose et al., 1999*; *Ozawa et al., 2001*; *Miyazaki et al., 2002*], the Cascadia subduction zone [*Dragert et al., 2001*], and beneath Kilauea volcano in Hawaii [*Cervelli et al., 2002*]. The moment magnitudes of these events range from $M_W 5.7$ beneath Kilauea to nearly $M_W 7$ in the case of the two subduction zone events. The durations of these events also vary considerably. The Bungo Channel event in southwest Japan lasted roughly one year, the Cascadia silent earthquake approximately 6 weeks, while the Kilauea silent slip event had a duration of roughly two days. Previously, slow earthquakes have been identified from strain and creep recordings [*Linde et al., 1996*]. Transient post-seismic deformation is also well established [e.g., *Heki et al.,* 1997; *Donnellan and Lyzenga,* 1998; *Segall et al.,* 2000].

Of course, deformation in volcanic regions is well known to be episodic [e.g., *Dvorak and Dzurisin,* 1997]. Transient deformation precedes some, if not all, volcanic eruptions. The time scales of the pre-eruptive deformation, however, can be quite variable. For example, permanent GPS stations on Kilauea volcano recorded 8 hours of extension prior to a rift eruption in 1997 [*Owen et al., 2000*]. On the other hand, a network of borehole strainmeters showed transient motion only 30 minutes prior to a basaltic eruption of Hekla in Iceland [*Linde et al., 1993*]. Long-term inflation is also seen prior to eruption of many shield volcanos. Recent evidence from InSAR shows signs of inflation episodes on numerous Aleutian volcanos [e.g., *Lu et al., 2000*].

While past results are certainly not promising, it is not inconceivable that deformation transients might precede earthquakes. Given the tremendous investment in building permanent GPS networks and collecting INSAR data, it is imperative that we explore these data fully to reveal the underlying fault-slip process. In particular, given data from frequently sampled, dense geodetic networks, it is now possible to address questions such as: "Does the pattern of aseismic slip-rate change before large earthquakes?" "What is the space-time evolution of silent earthquakes; i.e., what are characteristic rupture velocities and rise times, and what does this reveal about fault zone processes and constitutive properties?"

In this proposal we focus on data from the SCIGN network in southern California and the GEONET in Japan. The installation of the Southern California Integrated GPS Network (SCIGN), consisting of 250 continuously operating GPS stations was completed in June of 2001, and is producing high quality deformation data. Analysis of the SCIGN data is proceeding at JPL (under the direction of Dr. Hurst), and independently at Scripps. The data are currently being analyzed to produce daily values of station position with repeatabilities in the range of 1.5 mm horizontally, and 3-4 mm vertically. Results are available to the community via the web at http://milhouse.jpl.nasa.gov/scign/analysis and http://sopac.ucsd.edu/projects/scign/.

SCIGN station velocities have been combined with campaign, GPS, VLBI, and Geodolite distance observations in the SCEC velocity solution for southern California. The SCEC velocity field clearly shows the distribution of deformation across the North America - Pacific plate boundary (Figure 1). A large part of the deformation is elastic strain associated with the major strike-slip faults of the San Andreas fault system, although a significant portion is related to thrust faulting in the Transverse Ranges and Los Angeles Basin. Several investigators have developed dislocation models based on these data for all, or part of, Southern California [e.g., *Feigl et al.*, 1993; *Argus et al.*, 1999; *Shen et al.,* 1996]. To date, these studies have estimated the steady slip-rate and locking depth on faults in southern California, or have modeled recognized post-seismic transients. There has been little systematic effort devoted to detection of subtle transients.

One of the primary goals of the SCIGN network is to examine and understand time-dependent deformation of the earth's crust associated with the earthquake cycle in Southern California. There is abundant evidence of clustering of seismicity, and considerable debate over the existence, causes, and mechanisms of stress transfer from one rupture area to other future rupture areas.

GPS data show clear evidence of post-seismic strain transients following the Landers [*Shen et al.,* 1994], Northridge [*Donnellan,* 1998], and Hector Mine [*Owen, et al.,* 2001] earthquakes (e.g., Figure 2). The existence of transient tectonic deformations not following earthquakes is much more controversial. Nevertheless, there is evidence in the data for non-steady motions. Figure 3 shows the time series for station ELSC, which exhibits a transient signal around 2000.25 in both horizontal components. At this point we can not be sure whether this is tectonic or due to monument instability. With 250 stations producing data, it has not been possible to manually scan the data to identify motions which are coherent across multiple stations, and to distinguish between tectonic processes and, for example, groundwater induced deformations. This proposal will provide a tool to allow us to automatically scan the data on a regular basis, identifying coherent deformation caused by slip on faults.

The other principal source of GPS data for this project will be the Japanese GEONET (GPS Earth Observation Network). The Geographical Survey Institute of Japan (GSI) began to operate this nationwide GPS network on October 1994 [*Tsuji et al.*, 1995]. The network was expanded to a denser network consisting of 610 permanent stations on April 1996. An outline of the daily analysis strategy is found in *Miyazaki and Heki* [2001]. The entire data set is divided into three subnetworks based on different antenna-receiver types. Each subnetwork is processed separately using Bernese version 4.1β software. GSI utilizes precise orbit information and earth rotation parameters provided by the International GPS Service (IGS). The orbit and earth rotation parameters are fixed to their *a priori* values, and station positions are estimated together with tropospheric zenith delays every three hours. The three subnetworks are combined by tightly constraining (at the 0.1 mm level) three GPS stations in Tsukuba, which are present in all three subnetworks. This procedure is certainly sub-optimal in that it prevents one from determining the correlations between stations in the separate subnetworks. In our work with these data to date, we have "deconstrained" the GEONET solutions to obtain quasi-fiducial free solutions. Details are given in [*Miyazki et al.*, 2002].

The GEONET data have already revealed fascinating results. The average site velocities have been modeled by a number of groups. For example, *Mazzotti et al.,* [2000] analyzed GEONET data to determine the degree of locking along the Nankai trough and Japan trench. While they find several weakly coupled areas, both subduction zones are nearly completely locked. *Heki et al.* [1997] found that afterslip following the 1994 Sanriku earthquake in NE Japan, exceeded the moment released in the earthquake. Even more surprising, a silent thrust event with a duration of roughly one year was observed in SW Japan, where the Philippine Sea plate subducts beneath the Japan arc [*Hirose et al.*, 1999; *Ozawa et al.*, 2001; *Miyazki et al.*, 2002]. This remarkable transient is discussed in more detail below.

For this project we will focus on the Tokai area, which is thought to represent a significant seismic gap [*Ishibashi*, 1981]. In Suruga Bay the Philippine Sea plate subducts beneath the Eurasian plate. To the south on the Nankai Trough, major earthquakes occurred in 1944 (Tonakai, M7.9) and 1946 (Nankai, M8.0), however a major earthquake has not occurred in Suruga Bay since the 1854 Ansei-Tokai earthquake. The demonstrated capability of a major earthquake, the 140 year quiescence, and the proximity to metropolitan Tokyo have made the Tokai gap the focus of earthquake prediction efforts in Japan.

Beginning in mid 2000 GEONET stations in the Tokai area began to record anomalous and accelerating crustal deformation [*Fujii et al.*, 2001]. Anomalous motions are exhibited at numerous stations (Figure 4) and in completely independent leveling data (this can not be a local site effect, reference frame, or orbit problem), but is restricted to the Tokai region. Preliminary analysis using an early form of the Network Inversion Filter suggests that the deformation can be modeled by accelerated slip on the down-dip portion of the subduction interface (that is below the expected seismogenic zone) [*Ozawa et al.*, 2001]. Although their results were heavily smoothed, both spatially and temporally, the latter authors find that the total moment released by 2001.8 is 12 $\times 10^{18}$ N-m, in excess of Mw 6.6. There is even a suggestion that similar events have occurred in the past, although they were not recognized at the time [*Kimata et al.*, 2001].

There are major challenges in developing time dependent inverse methods for transient changes in slip-rate. First, we do not know *a priori* the nature of the temporal variations that we are trying to detect. Secondly, space geodetic measurements contain spatially and temporally correlated errors, due to atmospheric path delays and, multipath, and random benchmark motions [e.g., *Wyatt*, 1989]. Thus, any viable estimation procedure must allow for general, non-parametric estimation of the temporal variations in fault slip, and account for correlated errors in the observations. Temporally correlated errors with known stochastic properties, which are not present in the analogous seismic inverse problem, require the development of an appropriate inversion formalism for geodetic time series. Thirdly, due to imperfect resolution of the data, any inversion procedure will involve some spatial and temporal smoothing. It is very desirable that the amount of smoothing be determined by some rigorous procedure, not simply the analysts prejudice about what the slip-distribution should look like.

Our approach is based on previous work of *Segall and Matthews* [1997] and is referred to as a Network Inversion Filter (NIF). The NIF marries linear time-domain filtering with spatial inverse methods. *Segall et al.* [2000] showed how to separate spatial and temporal smoothing by implementing the spatial smoothing through pseudo-observations. This method has been applied to the postseismic deformation following the 1989 Loma Prieta Earthquake [*Segall et al.*, 2000], the 1999 Izmit earthquake [*Burgmann et al.*, 2001], and volcanic deformation accompanying the 1997 dike intrusion beneath the Izu peninsula in Japan [*Aoki et al.*, 1999]. In our recent work on the Bungo Channel silent thrust event we allow for reference frame errors in the GPS data in the observation equations [*Miyazaki et al.*, 2002].

We model GPS station positions relative to an *a priori* estimate $\mathbf{X}(t)$, as a function of time t, as

$$\mathbf{X}(t) = \sum_k H(t - t_{eq(k)})\mathbf{X}^{cos(k)} + \int_A s_p(\boldsymbol{\xi}, t - t_0) G^r_{pq}(\mathbf{x}, \boldsymbol{\xi}) \mathbf{n}_q(\boldsymbol{\xi}) dA(\boldsymbol{\xi}) + F\mathbf{f}(t) + L(\mathbf{x}, t - t_0) + \boldsymbol{\epsilon} \quad (1)$$

where the first term on right hand side represents coseismic offsets $\mathbf{X}^{cos(k)}$ at times $t_{eq(k)}$, where $H(t)$ is a Heavyside function. The second term on the right hand side represents deformation due to transient aseismic slip. We relate the time dependent site motions to slip on faults in an elastic medium as a function of position $\boldsymbol{\xi}$ and time, $s_p(\boldsymbol{\xi}, t-t_0)$ through Green's functions $G^r_{pq}(\mathbf{x}, \boldsymbol{\xi})$. To date, Green's functions relating slip to surface displacement have been computed using analytical expressions for dislocations in uniform half-spaces, although there is no impediment to computing Green's functions in heterogeneous or layered media. In (1) p, q, r = 1,2,3, and summation on repeated indices is implied, $\mathbf{n}_q(\boldsymbol{\xi})$ is the unit normal to the fault surface $A(\boldsymbol{\xi})$.

In (1) the fault slip includes both stead-state and transient components. In some cases where modeling the steady-state deformation field is not possible (at least to sufficient accuracy), we have found it useful to separate the steady station velocities by adding a term $\mathbf{V}_{sec} \cdot (t-t_0)$ to (1). In this case s_p in (1) represents only the transient component of fault slip. Given sufficient data it is possible to estimate the secular velocity $\mathbf{V}_{sec}$ along with the transient fault slip. In other cases we have estimated $\mathbf{V}_{sec}$ separately and subtracted it from the position time series prior to filtering.

The remaining terms are related to measurement and reference frame errors. The term $F\mathbf{f}(t)$ represent reference frame errors, where F is a linearized Helmert transformation and $\mathbf{f}(t)$ is a vector of rigid body translation, rotation, and scale factor. The fourth term on the right hand side of (1), $L(\mathbf{x}, t-t_0)$, represents random benchmark wobble, which we model as a Brownian random walk with scale parameter τ (units length/time$^{1/2}$) [*Wyatt*, 1989]. While some studies have advocated a flicker noise model for benchmark motion [*Mao et al.*, 1999; *Zhang, et al.,* 1997], *Langbein and Johnson* [1997] using over 10 years of data show that a random walk fits the data quite well. Without a long time series it is very difficult to distinguish between flicker noise (with a $1/f$ spectral decay) and random walk (with a $1/f^2$ spectral decay). A key feature of the Network Inversion Filter is that it can distinguish spatially correlated transient signal from site specific colored noise. The reason for this is that elastic deformation causes a spatially coherent signal, whereas the local benchmark motions are, by definition spatially incoherent. The fact that the local benchmark motions are spatially incoherent may be more important than the precise form of the spectral decay.

The final term $\boldsymbol{\epsilon}$ represents observation error, which we take to be normally distributed with zero mean and covariance $\sigma^2\Sigma_{\mathbf{x}}$, where $\Sigma_{\mathbf{x}}$ is the covariance matrix of the GPS positions, and σ^2 is a scale factor to account for unmodeled errors such as mulitpath, or azimuthally varying path delays.

The earliest inversions using the NIF (cited above) suffered from two problems. First, the linear Kalman Filter did not allow for non-negativity constraints. It is well established in time independent inversions that the addition of non-negativity constraints (e.g., prohibiting left-lateral slip on the San Andreas Fault) substantially improves spatial resolution. Secondly, the spatial and temporal smoothing parameters were determined by Maximum Likelihood. Using a prediction error decomposition, *Segall and Matthews* [1997] showed that the likelihood could be computed using a recursive filter that inverted the state-covariance matrix at each epoch. While relatively fast, compared to inverting the full data covariance matrix, this approach proved to be computationally burdensome – the full data set needed to be run through a forward filter for every choice of smoothing (hyper) parameters.

Recent work, detailed in *McGuire and Segall* [in prep], has substantially improved on previous methods. Firstly, we have implemented a non-linear, extended Kalman Filter, that allows non-negativity constraints to be applied. We have found that this substantially improves the spatial resolution of the inversions. Secondly, we include the smoothing (hyper) parameters in that state vector and estimate them directly in the filter. This avoids the computationally costly maximum likelihood procedure. Synthetic tests indicate that this procedure leads to nearly optimal choices of the smoothing parameters. Details of the inversion procedure are omitted here for brevity. Rather we show results of time dependent inversions using data from southwest Japan and the Cascadia subduction zone.

From late 1996 to late 1997 aseismic slip on the Philippine Sea plate subduction interface beneath Kyushu and Shikoku islands produced large transient deformation signals which began as afterslip subsequent to the two M_W 6.7 Hyuga-nada earthquakes (Figure 5). The afterslip was then followed by the Bungo Channel slow earthquake centered 100 km further north [*Hirose et al.,* 1999; *Ozawa et al., 2001*]. The inversions of *Ozawa et al.*, [2001] show that the afterslip propagated from south to north into the Bungo Channel area. However, the authors suggest that this is an artifact of over-smoothing in their analysis. In contrast, our results [*Miyazaki et al.,* 2002], including non-negativity and automatic determination of temporal and spatial smoothing parameters, demonstrate that the afterslip and the Bungo Channel silent earthquake were separated by a 50 km long region of little to no slip (Figure 5). The peak slip in both events occurred between depths of 35 and 50 km. Note from Figure 5 that stations near the Bungo Channel show coherent transient motions beginning in mid 1997. Peak slip rates were ∼1 m/yr in the afterslip event and ∼2 m/yr in the Bungo channel event. The Bungo Channel slow earthquake nucleated on the shallow portion of the thrust interface and propagated to greater depth.

In 1999 the Cascadia subduction interface beneath Seattle and Vancouver Island ruptured in an aseismic slip transient that lasted about 6 weeks [*Dragert et al.*, 2001]. This event produced surface displacements of up to ∼ 4 mm at GPS sites in the area. Inversion of the available data demonstrates that the event nucleated at a depth of around 30 km and propagated dominantly along-strike to the north as well as slightly updip (Figure 6). The slip rise-time at any point on the fault is much shorter, (1-2 weeks), than the Bungo Channel event (months), and peak slip-rates were ∼ 0.5 m/yr. Our estimated slip distribution [*McGuire and Segall*, in prep] implies a significantly higher stress-drop than the slip distribution determined through forward modelling by *Dragert et al.* [2001]. Our study found slightly (∼ 20%) larger displacements at several stations resulting from fault-slip than the forward modelling study did. This primarily results from simultaneously estimation of a non-parametric, stochastic description of local site motion as opposed to removing a parametrized "seasonal" signal before estimating the surface displacements associated with the slow event. This event demonstrates both the need for properly parameterized inversion studies and the fact that magnitude 6+ slip events can easily "hide" undetected in modern datasets despite dense spatial coverage.

Animations showing fault slip-rate for both the Bungo Channel and Cascadia slow earthquakes can be accessed from

`http://kilauea.stanford.edu/~jeffmcgu`

2.2 Proposed Work

We propose to complete development of time-dependent inversion methods for space geodetic data. These inversions provide full space time history (essentially 'movies') of slip-rate on faults. We will also develop automated procedures for detecting changes in deformation without specifying the details of the causative structures. That automated methods are required is obvious when one considers that a 1000 station array generates nearly one million three-dimensional position determinations per year. It is not possible for an individual to hope to detect subtle transient events in a data set of this size.

To advance our ability to invert continuous geodetic data for information about time-variable deformation processes, we propose the following four activities:

1. Completion of the Network Inversion Filter.

2. Development of the Network Strain Filter (NSF) for monitoring large regions and detecting deformation transients.

3. Application of the NSF and NIF to the SCIGN dataset, representing the first coherent attempt at extracting time variable information in southern California.

4. Application of the Network Inversion Filter to the aseismic deformation episode ongoing in the Tokai Gap in Japan. This represents the best dataset yet recorded of a large Mw 7+ transient downdip of a locked megathrust.

We note that these tasks support NASA's long term goal of developing forecasting techniques for mitigating earthquake risk. Specifically, we support the utilization of data from the SCIGN network and other large scale GPS arrays, and the development of geodetic techniques for improved understanding of the nature and dynamics of magmatic plumbing systems.

2.2.1 Completion of the Network Inversion Filter

Much of the work on the extended Network Inversion Filter is complete. However, in order to make this tool more widely applicable we plan to:

(1) Explore effects of spatially variable random walk variance. To date we have assumed that all sites have statistically similar behavior. Yet it is almost certain that some sites are noisier than others. With the advent of the extended NIF it is possible to include separate variance parameters for individual stations, or for groups of stations. For example, all bedrock sites might be grouped

together. It may also be possible to estimate these variance parameters from "quiet" parts of the GPS time series.

(2) Explore possibility of incorporating InSAR results with GPS data. One of the nice features of the Kalman Filter is that there is no requirement that the size of the data vector be constant from epoch to epoch. It is thus straightforward to incorporate campaign GPS data along with continuous observations. It should also be possible then to include InSAR data in the analysis. The advantage of such an approach is clear: InSAR provides unprecedented spatial resolution, but (at least at present) limited temporal resolution. Combining GPS and InSAR then could provide substantially enhanced spatial resolution from GPS data alone. The challenge is that we need to know the covariance structure of the InSAR data. While considerable work has been done on this problem [e.g., *Hanssen,* 2001; *Jonsson, et al.* 2001], it is by no means solved. We will collaborate with Prof H. Zebker (Stanford) who is submitting a separate proposal in response to this NRA to focus on this important issue.

(3) Produce distributable software for other users. We have been asked by several groups for Network Inversion Filter software. Until recently, we felt that the code was not sufficiently well developed to distribute. Many of the issues have recently been worked out and it is now time to make accessible code available to NASA and other researchers. This will be a time consuming task, as the code now consists of a large number of matlab routines that, in many cases, are customized to particular data sets.

2.2.2 Development of a Network Strain Filter

Time domain filtering methods are not only able to estimate past fault-slip histories, they also lead rather naturally to anomaly detectors. As discussed previously, it can be difficult to synthesize data from an array of stations by eye to infer changes in the underling fault-slip process, particularly when networks contain hundreds to thousands of stations. It is clear that automated procedures are needed to assess whether changes in the style of crustal deformation have taken place. Time domain filtering is ideal for this because the filter is continually predicting the next state, conditioned on all past data, and then comparing with the next set of observations. When the new data differs significantly from the prediction this is a natural indicator of a change in the underlying process.

There are many places where space geodetic networks are so broad that it will be difficult to model all the structures that might be contributing to the contemporary deformation field. In these situations it is desirable to have a filter that does not demand one know the detailed geometry of all faults and magma bodies in the area. Such a method should be able to detect time varying strain at a range of spatial scales. Once detected, one could compute Green's functions for the NIF assuming the active structures in the vicinity of the anomalous deformation are reasonably well known.

An alternate approach, which we refer to as a Network Strain Filter (NSF), is to model the data in terms of a spatially and temporally variable deformation field. If we replace the integral representation of the displacement due to fault slip with a general spatially and temporally variable displacement $\mathbf{u}(\mathbf{x},t)$, then equation (1) becomes

$$\mathbf{X}(t) = \sum_k H(t - t_{eq(k)})\mathbf{X}^{cos(k)} + \mathbf{u}(\mathbf{x},t) + F\mathbf{f}(t) + L(\mathbf{x}, t - t_0) + \boldsymbol{\epsilon} \tag{2}$$

Expanding $\mathbf{u}(\mathbf{x},t)$ in terms of spatial basis functions $B_n(\mathbf{x})$ we have

$$u_i(\mathbf{x}, t) = \sum_k^K B_k^{(i)}(\mathbf{x}) c_k^{(i)}(t) \tag{3}$$

where the index $^{(i)}$ refers to the component of displacement and the index $_k$ refers to order in the expansion.

Assuming that the basis is differentiable, we can compute the strain and rotation from the gradient of the displacement,

$$\frac{\partial u_i(\mathbf{x}, t)}{\partial x_j} = \sum_k^K \frac{\partial B_k^{(i)}(\mathbf{x})}{\partial x_j} c_k^{(i)}(t). \tag{4}$$

Note that for large networks it will be necessary to use geodetic coordinates (θ, ϕ, h), (lat,long, height). Strains on the sphere are given by Love (1944) in terms of the geodetic displacements.

Careful consideration needs to be given as to the appropriate choice of basis functions. Several obvious choices are probably not well suited to this problem. For example spectral bases, i.e, spherical harmonics, have global support (are non-zero over the entire domain) and thus require many terms to represent a localized process. Yet we need the capability of detecting a localized deformation source (say a volcanic inflation, or buried fault slip) in a large geodetic array like GEONET. The other drawback to a spectral basis is that, again because of the global support, data errors in one location effect the estimation globally. Other bases that warrant investigation include splines and wavelets. The appealing attribute of wavelets is that they have local support (are non zero only in a small domain) and thus can efficiently represent a localized function.

There has been considerable work done on wavelets defined on a spherical domain (e.g. Schroder and Sweldens, 1995). For example, Hansen (2002) discusses inversion of GPS delay measurements for the spatial and temporal distribution of free electron density in the ionosphere. He examines a number of basis functions including both separable and non-separable wavelets. The simplest approach is to take a separable basis, and represent displacements on the sphere as the tensor product of wavelets in latitude and longitude

$$B(\theta, \phi) = \{\Psi(\theta) \otimes \Psi(\phi)\} = \left\{ \prod_{mns}^{MNS} \Psi_m^s(\theta) \Psi_N^s(\phi) \right\} \tag{5}$$

where s is the wavelet scale. The wavelet basis is defined by a mother wavelet at the largest scale; wavelets at smaller spatial scales are determined by translations and dilations of the mother wavelet. The largest spatial scale in this case is the scale of the geodetic network. The smallest scale will depend on the density of stations. We insist that at the smallest scale the wavelet cover some minimum number of stations. This ensures that time-varying deformation is separable from local benchmark motions. We will investigate various wavelets, including non-separable wavelets, for this application. Note that the simplest, Haar, wavelet is non-differentiable and thus not suited for this application. Finally, care will be required if there are creeping faults, in which case the assumption of differentiability will be violated.

Combining equations (2), (3), and (5) yields the Network Strain Filter. As in the NIF, we will employ a stochastic representation of the coefficients $c_k(t)$. Thus, the coefficients c_k and their time derivatives, as well as the local benchmark motions, and coseismic offsets appear in the state vector. Time domain filtering of the type we have implemented in the NIF will then yield estimates of the parameters. From these the variation in strain as a function of space and time can be constructed from the derivatives as in (4). It should be emphasized that this is an entirely new type of filter that can be applied to any regional continuous geodetic network, whether or not we have the necessary information to parameterize all the active deformation structures. We anticipate that this tool will be widely applied to different data sets in search of subtle time varying strains. Once detected these interesting signals can be the subject of more specific modeling using the NIF or other tools.

2.2.3 Application to SCIGN data

Visual examination of the SCIGN data suggest that there may be time-varying deformation that is not explained by current models. Without evidence for clear spatial coherence of these motions we can not be sure that the observed transients are tectonic. Our analysis of the SCIGN data will thus proceed along two tracks. First, we will employ the NSF to search for spatially coherent strain changes within the SCIGN data set. Presently, the only well documented transients are associated with postseismic deformation following the Landers, Northridge, and Hector Mine earthquakes. We will use the NSF to search for more subtle changes in the character of the deformation field. If any apparent changes are found we will examine the data and data processing to ensure that artifacts have not been introduced. Areas that appear to exhibit anomalous deformation can be examined more thoroughly with a fault specific NIF.

In order to apply the NIF to SCIGN data we require a kinematic model of the active faults within the region, including both the fault geometry and steady interseismic slip rates. Fortunately, we can make use of other efforts, including SCEC community fault models, the latest SCEC crustal velocity model, and the GEM (General Earthquake Modeling) initiative to develop a database of fault parameters. We plan to begin with the 1996 CDMG fault model [*Petersen et al.* 1996], which provides a 3D tiling of the active faults in California with 183 segments. We also hope to make use of improved models being developed by GEM, the RELM (Regional Earthquake Likelihood Model) and the SCEC communities which will become available during the lifetime of this project.

Given the fault geometry, and the SCEC crustal velocity model (Figure 1), we will construct a first order dislocation model of southern California. Here, we can build on the work of *Feigl et al.* [1993], *Donnellan et al.* [1993], *Shen et al.* [1996], and *Argus et al.* [1999], among others. *Feigl et al.,* [1993] used GPS (1986-1992), and VLBI (1984-1991) data to estimate a velocity field for Southern California. They modeled this velocity field using dislocations to represent the principal faults locked below a specified depth. The residual velocity field showed deformation rates of 2-5 mm/yr in the Santa Barbara Channel, the Ventura and Los Angeles basins, the Santa Maria Fold and Thrust Belt, the Temblor Range north of the Big Bend, and between the offshore islands and the mainland south of the Transverse Ranges. *Shen et al.* [1996] used GPS, trilateration, and triangulation measurements to estimate interseismic station velocities in the greater Los Angeles region. They also pointed out that the deformation pattern can not be explained by motion solely on the San Andreas fault. *Donnellan et al.,* [1993] focused on the Ventura basin, demonstrating that the observed deformation pattern could be explained by slip below a shallow locking depth on the two basin bounding faults. *Argus et al.,* [1999] examined the convergence observed in GPS data spanning the Los Angeles Basin from Palos Verdes to the base of the San Gabriel Mountains. Given the low observed rate of east-west extension, they concluded that the north-south convergence must be accommodated by crustal thickening.

In contrast to earlier studies outlined above, the work we propose will result in a comprehensive estimate of the *time-dependent* slip rate on all the candidate faults that we identify in the region. We can use the estimated average interseismic slip-rates on the candidate faults (and associated covariance matrix) from the SCEC velocity field as a prior to initiate the NIF. Alternatively, we can simply estimate the steady-state velocities of the SCIGN stations $\mathbf{V}_{sec}$, simultaneously with the *transient* fault slip-rates. The latter approach eliminates potential biases due to mis-modeling of the secular deformation field. It should be emphasized that either approach is only recently viable due to the availability of the dense and continuous SCIGN data and will represent a significant advance in our ability to understand the details of the Southern California deformation field.

Detecting time varying deformation in the SCIGN data will be complicated by the presence of spatially coherent signals from fluctuations in ground water. The water district in Orange County has started managing the underground aquifers there as storage reservoirs, putting water into them when available, and pumping water out of them during dry seasons. As a consequence, many of the GPS stations in the region show large (cm level) movements which are clearly due to ground water effects. This phenomenon is not limited to Orange County, though it is most systematic and widespread there [*Bawden et al.*, 2001]. Methods will need to be developed to account for this phenomenon. Solutions may be as crude as throwing out data clearly contaminated by ground water. It may also be possible to reduce this effect by specifically including information from water pumping records in our analysis [e.g., *Segall,* 1992].

Other deformation measurements being made in Southern California include InSAR, and strain measurements. InSAR deformation maps provide unparalleled coverage, but are infrequently sampled. Borehole and long-baseline surface strain provide deformation data with lower noise than

GPS at periods shorter than about 1 month. Depending on the success of our work, we hope to incorporate strain and InSAR data into our NIF analysis. InSAR would enhance the spatial resolution, while strain significantly improves our sensitivity to short term fluctuations in fault slip. As is the case with InSAR measurements, the main difficulty is in determining the proper covariance structure of the data.

One of the main goals of the SCIGN network is the identification of time-variant deformation signals related to earthquakes. To be most useful, such signals should be identified in as near real-time as possible to allow investigation using other instruments, and also more informed decision making by planning personnel. Initially, the main thrust of this proposal will be to use the daily station coordinates as input to the NIF analysis. Subsequently, we will include the ability to use data from long baseline and borehole strain instruments.

2.2.4 Application to GEONET and Tokai gap

The second area we will study is the Tokai seismic gap region in Japan. The evidence for ongoing transient deformation there has already been discussed. Given the extreme risk associated with a Tokai earthquake, a crucial question is: Is the anomalous motion a prolonged silent earthquake, similar to the Bungo Channel event? Or is it (unlikely) an accelerating process that will lead to a major earthquake? The largest subduction zone earthquake ever recorded, the 1960 Chile M_w 9.5 (?) Chile event, began with an episode of smooth slow slip that lasted at least several hundred seconds before triggering the destructive mainshock [*Kanamori and Cipar*, 1974;*Cifuentes and Silver*, 1989]. This slow slip, which was itself $M_w \sim 8\frac{1}{2}$, occurred downdip of the mainshock seismogenic zone [*Linde and Silver,* 1989]. Thus, understanding aseismic slip transients on the deeper portion of a subduction interface is important in the earthquake process owing not only to the "prestress" conditions imposed on the seismogenic zone but also because in some cases it may represent the beginning of the seismic nucleation process. There are two critical parameters that need to be constrained to describe the effect of the aseismic slip on the seismogenic fault, the spatially variable stress drop during the slow event and its rise-time at any one point. These quantities determine both the stress change on the seismogenic region and the associated strain-rate, the time-dependent quantities needed to constrain fault friction-laws. The resolution of these quantities is directly tied to the details of the estimation technique. Studies of the Tokai event with the older version of the NIF [*Ozawa et al.,* 2001] have been unable to resolve the extent slip and the propagation direction, owing to the oversmoothing necessary to enforce positivity in that formulation. Given the exceptional spatial density of geodetic data in this area (station spacing of $\sim$ 30 km), the combination of this dataset with the latest version of the NIF represents the best opportunity to date to characterize the detailed space-time history of a slow-slip event and hence the parameters that can help constrain fault-zone rheology.

For this component of the study, we will collaborate with Dr. Teruyuki Kato and Dr. Shinichi Miyazaki of the Earthquake Research Institute, University of Japan, and Dr. Takeshi Sagiya and

Dr. Hatanaka of the Geographical Survey Institute of Japan. Through our collaboration with scientists at ERI and GSI we have recently begun the process of setting up the latest version of the NIF to work with the available Tokai dataset. We are also exploring the possibility of running the NIF on the Tokai data in near realtime to aid in hazard estimation.

2.3 Figures

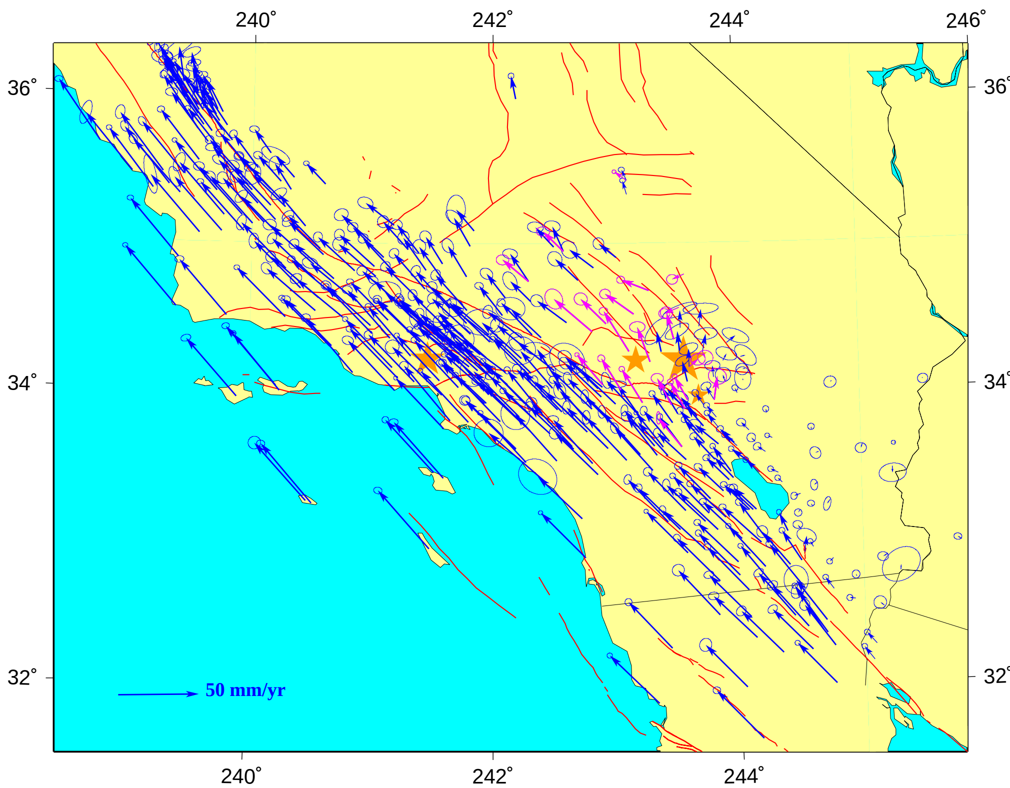

Figure 1: SCEC velocity field in southern California, courtesy of www.scec.org.

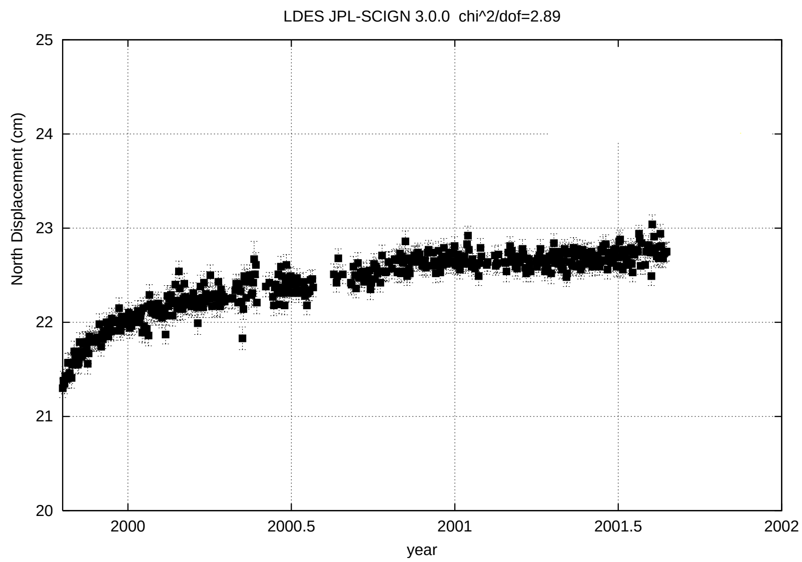

Figure 2: North component of motion at the SCIGN station LDES, the Landers Elementary School. A clear post-seismic transient from the Hector Mine earthquake is visible. Only the north component for LDES is shown for clarity. Other components show similar signatures, but at a smaller amplitude.

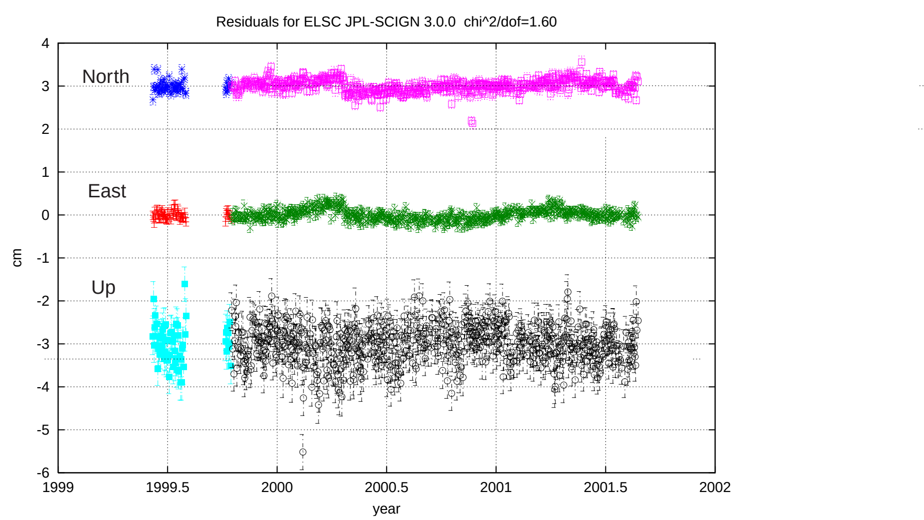

Figure 3: East, north, and vertical components of motion at ELSC, a SCIGN station at the East Los Angeles Science Center. The time varying signature at this station could be due to motion on faults, groundwater fluctuations due to pumping of local aquifers, or unattributed local benchmark motion. Understanding the origin of such signals is one of the primary goals of this proposal.

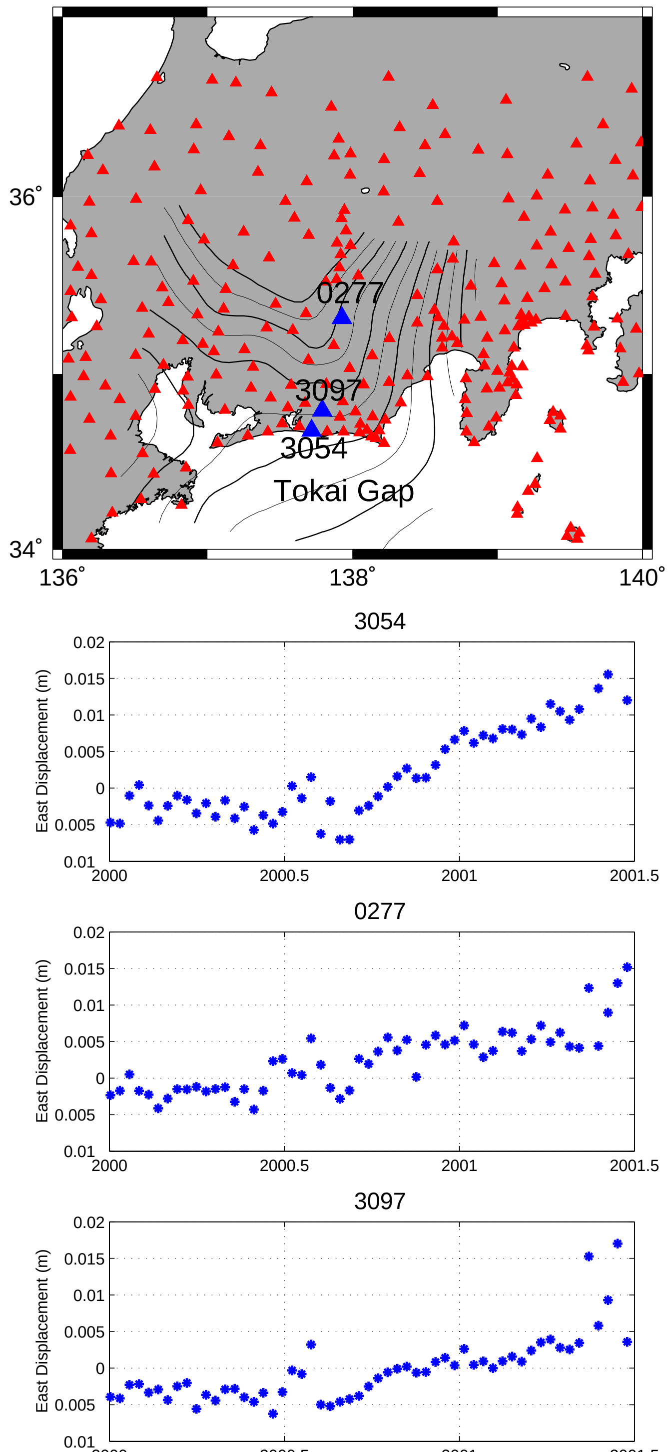

Figure 4: Map showing the Tokai seismic gap region of Japan. Red triangles indicate GPS stations. Blue triangles stations for which time series are shown. Contours show estimates of the top of the subducting Philippine Sea plate. The time series show preliminary results from the Network Inversion Filter in which the secular trend, reference frame, and benchmark wobble terms have been removed.

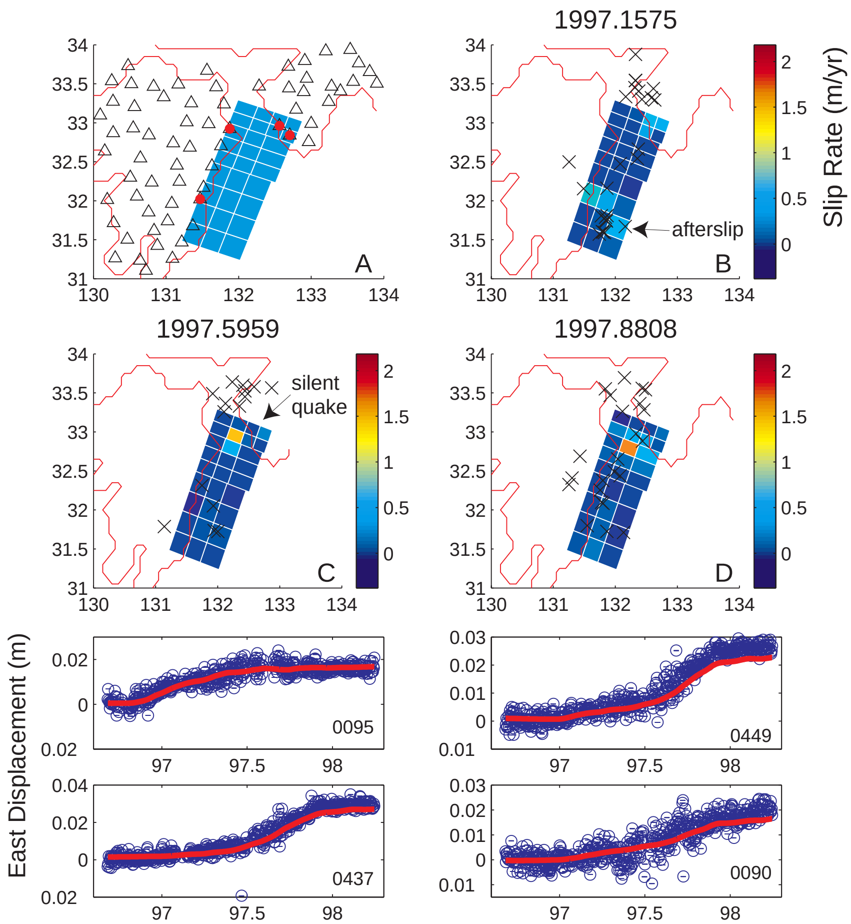

Figure 5: Results of applying the Network Inversion Filter to the GPS data recorded on Shikoku and Kyushu islands from late 1996 to early 1998. Panel A shows the fault geometry (colored rectangles), the coastline (red line) and the GPS stations used in the inversion (triangles). Red circles denote the locations of the stations shown in the bottom panels. Panels B-D show the estimated slip-rate (colored rectangles) at three time periods in 1997 and earthquake locations (black Xs) during a ±3 day time period around the slip-rate estimate (B) Julian day 42, the Hyuganada afterslip in the south is clearly separated from the just nucleated Bungo Channel slow earthquake in the north. (C) Julian day 158, the afterslip has finished, and the Bungo Channel event has reached it's peak slip rates. (D) Julian day 233, the Bungo Channel event has propagated further south and will soon end. The bottom four panels show east component daily positions in m at the four stations highlighted in panel A. Estimates of the secular velocity, reference frame error, coseismic displacements, and benchmark wobble have been removed. The red lines indicate the fit to the data produced by our slip model for the slow events. Station 0095 is on the SE coast of Kyushu, 0090 is on NE coast of Kyushu, and both 0449 and 0437 are on the SE coast of Shikoku.

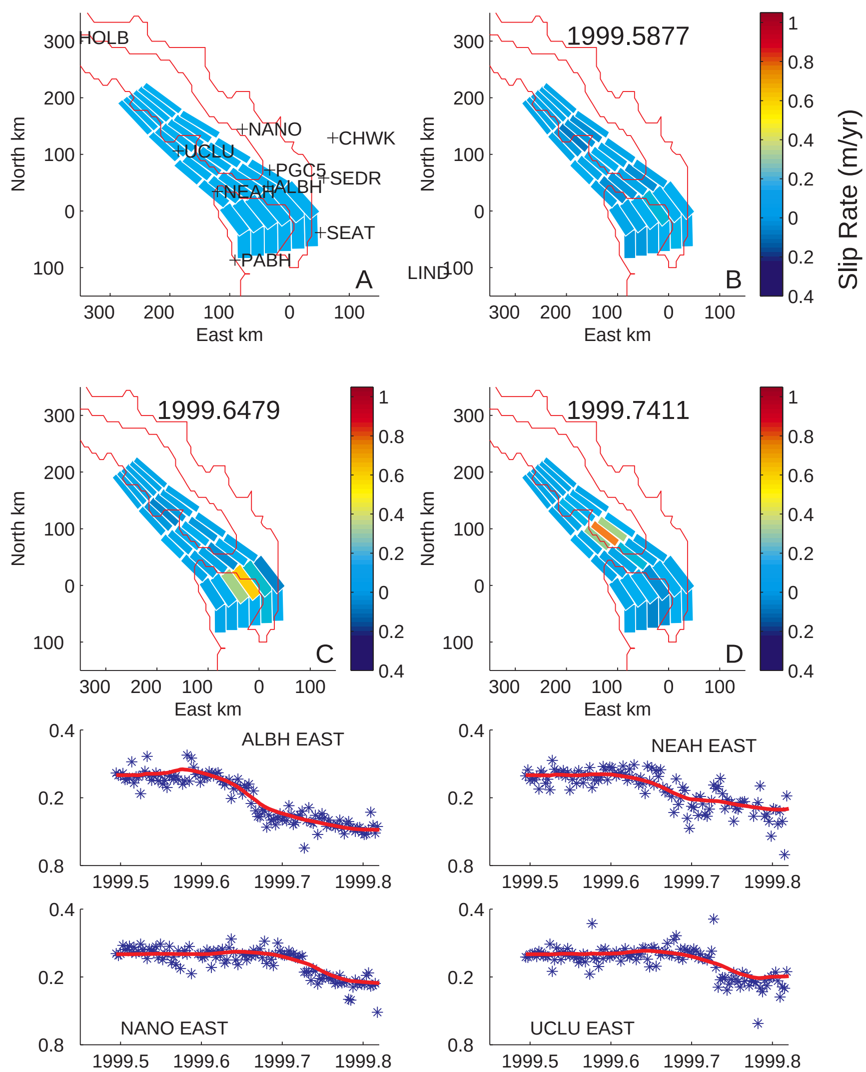

Figure 6: Results of applying the Network Inversion Filter to the GPS data recorded during the 1999 Cascadia subduction zone slow earthquake. Panel A shows the fault geometry (colored rectangles), the coastline (red line) and the nearby GPS stations. Panels B-D show the estimated slip-rate on the model subfaults (colored rectangles) at three time periods during the slow event. (B) Julian day 214, the slow earthquake has just nucleated. (C) Julain day 236, the rupture has propagated to the south and shallower. (D) Julian day 270, the rupture has propagated to the north and is about to end. The bottom four panels show east component daily positions in cm at four stations (blue stars). Estimates of the secular velocity, reference frame error, and benchmark wobble have been removed. The red lines indicate the fit to the data produced by our slip model for the slow event.

3 References

Aoki, Y., Paul Segall, Teruyuki Kato, Peter Cervelli, Seiichi Shimada, Imaging magma transport from inversion of deformation data: The 1997 seismic swarm off the Izu Peninsula, Japan, Science, vol. 286, 927-930, 1999.

Amelung F., S. Jnsson, H. Zebker, and P. Segall, Widespread uplift and trap door faulting on Galapagos volcanoes, Nature, v. 407 No. 6807 P. 993 996, 2000.

Argus, D., M. Heflin, A. Donnellan, F. Webb, D. Dong, K. Hurst, D. Jefferson, G. Lyzenga, M. Watkins, and J. Zumberge, Shortening and thickening of metropolitan Los Angeles measured and inferred by using geodesy, Geology, 27, 703-706, 1999.

Bawden GW, Thatcher W, Stein RS, et al. Tectonic contraction across Los Angeles after removal of groundwater pumping effects Nature 412 (6849): 812-815 Aug 23 2001

Bock, Y, Wdowinski, S, Fang, P, Zhang, J, Williams, S. Johnson H, Behr, J, Gengrich, J, Dean J, vanDomselaar M, Agnew D, Wyatt F, Stark K, Oral B, Hudnut K, King R, Herring T, Dinardo S, Young W, Jackson D, and Gurtner W, Southern California Permanent GPS Geodetic Array: Continuous measurements of regional crustal deformation between the 1992 Landers and 1994 Northridge earthquakes, J Geophys Res, 102 (B8), 18013-18033, 1997.

Burgmann, R., P. Rosen, E. Fielding, Synthetic aperture radar interferometry to measure Earth's surface topography and its deformation, Annual Review of Earth and Planetary Sciences, vol.28, pp.169-209, 2000.

Burgmann, R., Ergintav, S., Segall, P., Hearn, L., McClusky, S., Reilinger, R. E., Woith, H. Zschau, J., Time-space variable afterslip on and deep below the Izmit earthquake rupture, Bull. Seismosoc. Amer, in review, 2001.

Cervelli, P., P. Segall, K. Johnson, M. Lisowski, and A. Miklius, Sudden aseismic fault slip on the south flank of Kilauea volcano, Nature., in press, 2002.

Cifuentes, I. L, and P. Silver, Low-frequency source characteristics of the great 1960 Chilean earthquake, Journal of Geophysical Research, B, Solid Earth and Planets, vol.94, no.1, pp.643-663, 1989.

Donnellan A, Hagar BH, King RW, et al., Geodetic measurement of deformation in the Ventura-basin-region, Southern California, J Geophys Res-Sol EA 98 (B12): 21727-21739, Dec 10 1993.

Donnellan, A. and Lyzenga, G., GPS observations of fault afterslip and upper crustal deformation following the Northridge earthquake, J Geophys Res, 103 (B9), 21285-21297, 1998.

Dragert, H., K. Wang, and T. S. James, A Silent Slip Event on the Deeper Cascadia Subduction Interface Science, 292, 1525-1528, 2001.

Dvorak, J., D. Dzurisin, Volcano geodesy; the search for magma reservoirs and the formation of eruptive vents, Reviews of Geophysics, vol.35, no.3, pp.343-384, 1997.

Feigl K, Agnew DC, Bock Y, et al. Space geodetic measurement of crustal deformation in Central and Southern California 1984-1992, J. Geophys Res-Sol EA 98 (b12): 21677-21712, Dec 10 1993.

Fialko, Y., M. Simons, D. C. Agnew, The complete (3-D) surface displacement field in the epicentral area of the 1999 M_W 7.1 Hector Mine earthquake, California, from space geodetic observations, *Geophysical Research Letters*, vol.28, no.16, pp.3063-3066, 2001.

Fujii, N., H. Hirose, F. Kimata, F, and K. Hirahara, On-going Slow Slip Event at the Tokai Region, Central Japan, Eos Trans. AGU, 82(47), Fall Meet. Suppl., Abstract G31A-0128, 2001.

Hansen, A.J. Tomographic estimation of the ionosphere using terrestrial GPS sensors, Ph.D. Dissertation, Stanford University, 2002.

Hanssen, R. Data Interpretation and Error Analysis, Kluwer Academic Publishers, Dordrecht, The Netherlands, 308pp, 2001.

Heki, K., S. Miyazaki, and H. Tsuji, Silent fault slip following an interplate earthquake at the Japan Trench, *Nature, 386,* 595-598, 1997.

Hirose, H., K. Hirahara, F. Kimata, N. Fujii, and S. Miyazaki, A slow thrust slip event following the two 1996 Hyuganada earthquakes beneath the Bungo Channel, southwest Japan, *26,* 3237-3240, 1999.

Hudnutk, K., Y. Bock, J. Galetzka, F. Webb, and W. Young, The Southern California Integrated GPS Network (SCIGN), available at www.scign.org.

Hurst 2001: http://milhouse.jpl.nasa.gov/scign/analysis

Ishibashi, Katsuhiko, Specification of a soon-to-occur seismic faulting in the Tokai District, central Japan, based upon seismotectonics, Maurice Ewing Series, no.4, pp.297-332, 1981.

Jonsson, S., H. Zebker, P. Segall, InSAR Covariance Estimation, Data Reduction, and Combination of Multiple Datasets in Deformation Modeling, Eos Trans. AGU, 82(47), Fall Meet. Suppl., Abstract G31B-0140, 2001.

Kanamori, H, J.J. Cipar, Focal process of the great Chilean earthquake May 22, 1960, Physics of the Earth and Planetary Interiors, vol.9, no.2, pp.128-136, 1974.

Kimata, F., K. Hirahara, N. Fujii, and H. Hirose, Repeated Occurrence of Slow Slip Events on the Subducting Plate Interface in the Tokai Region, Central Japan, the Focal Region of the Anticipated Tokai Earthquake (M=8) Eos Trans. AGU, 82(47), Fall Meet. Suppl., Abstract G31A-0126, 2001.

Langbein, J., and H. Johnson, Correlated errors in geodetic time series: implications for time-dependent deformation, *102,* 591-603, 1997.

Linde, A. T. and P. Silver, Elevation changes and the great 1960 Chilean earthquake; support for aseismic slip, Geophysical Research Letters, vol.16, no.11, pp.1305-1308, 1989.

Linde, A., K. Agustsson, S.I. Sacks, R. Stefansson, Mechanism of the 1991 eruption of Hekla from continuous borehole strain monitoring, Nature (London), vol.365, no.6448, pp.737-740, 1993.

Linde, A., M. Gladwin, M. Johnston, R. Gwyther, and R. Bilham, A slow earthquake sequence on the San Andreas Fault Nature (London), vol.383, no.6595, pp.65-68, 1996.

Love, A.E.H., A Treatise on the Mathematical Theory of Elasticity, Dover, New York, 1944.

Lu, Z., C. Wicks, J. Power, and D. Dzurisin, Ground deformation associated with the March 1996 earthquake swarm at Akutan Volcano, Alaska, revealed by satellite radar interferometry, Journal of Geophysical Research, B, Solid Earth and Planets, vol.105, no.9, pp.21,483-21,495, 2000.

Mao, A., C.G.A. Harrison, and T.H. Dixon, Noise in GPS coordinate time series, J. Geophys. Res. *104,* 2797-2816, 1999.

Massonnet, D., M. Rossi, C. Carmona, F. Adragna, G. Peltzer, K. Feigl, and T. Rabaute, The displacement field of the Landers earthquake mapped by radar interferometry, *Nature* Vol. 364, pp. 138-142, 1993.

Mazzotti, Stephane, X. Le Pichon, P. Henry, Shin-Ichi Miyazaki, Full interseismic locking of the Nankai and Japan-west Kurile subduction zones; an analysis of uniform elastic strain accumulation in Japan constrained by permanent GPS, Journal of Geophysical Research, B, Solid Earth and Planets, vol.105, no.6, pp.13,159-13,177, 2000.

McGuire, Jeff and P. Segall, Imaging of aseismic fault slip transients recorded by dense geodetic networks, in prep.

Miller M. M., Johnson D. J., Rubin C. M., Dragert H., Wang K., Qamar A., Goldfinger C., GPS-determination of along-strike variation in Cascadia margin kinematics: Implications for relative plate motion, subduction zone coupling, and permanent deformation. Tectonics. v. 20, p. 161-176, April, 2001.

Miyazaki, S. and K. Heki, Crustal velocity field of southwest Japan: Subduction and arc-arc collision, Journal of Geophysical Research, 2001.

Miyazaki, Shin'ichi and P. Segall, A Transient Subduction Zone Slip Episode in Southwest Japan Observed by the Nationwide GPS Array, J. Geophys. Res., in review, 2002.

Murray, M. H. and P. Segall, Modeling broadscale deformation in northern California and Nevada from plate motions and elastic strain accumulation, Geophys. Res. Letters, in press, 2001.

Owen, S., P. Segall, M. Lisowski, M. Murray, M. Bevis, and J. Foster, The January 30, 1997 eruptive event on Kilauea Volcano, Hawaii, as monitored by continuous GPS, Geophysical Research Letters, v. 27, 2757-2760, 2000.

Owen, S., G. Anderson, D. Agnew, H. Johnson, K. Hurst, R. Reilinger, Z-K Shen, J. Svarc, and T. Baker, Early Postseismic Deformation from the Mw 7.1 Hector Mine Earthquake as Measured by Survey-Mode GPS, Submitted to BSSA March 16 2001.

Ozawa, S., M. Murakami, and T. Tada, Time-dependent inversion study of the slow thrust event in the Nankai trough subduction zone, southwest Japan, *106,* 787-803, 2001.

Ozawa, S., T. Murakami, M. Kaidzu, T. Tada, T. Sagiya, H. Yarai, and T. Nishimura, A Possible Precursor of an Anticipated Subduction Zone Thrust Earthquake in the Tokai Region, Central Japan, Detected by a Continuous GPS Network Measurements Eos Trans. AGU, 82(47), Fall Meet. Suppl., Abstract T52E-02, 2001.

Peltzer, G., P. Rosen, F. Rogez, and K. Hudnut, Postseismic rebound in fault step-overs caused by pore fluid flow, Science, Vol. 273, pp. 1202-1204, 30 August 1996.

Petersen, M. Bryant W., Cramer C., Cao T. Reichle, M., Frankel A., Lienkaemper J., McCrory P, and Schartz D., Probabilistic seismic hazard assessment for the State of California CDMG open-file report 96-08 1996. USGS open-file report 96-706 1996.

Schroder, P. and W. Sweldens, Spherical wavelets: Efficiently representing functions on a sphere, Computer Graphics Proceeding, SIGGRAPH, 1995.

Segall P., Induced stresses due to fluid extraction from axisymmetric reservoirs, Pure and Applied Geophysics, v 139, no 3/4, pp. 535-560, 1992.

Segall, P. and M. Matthews, Time dependent inversion of geodetic data, Journal of Geophysical Research., v. 102, p. 22,391-409, 1997.

Segall, P., R. Brgmann, and M. Matthews, Time-dependent triggered afterslip following the 1989 Loma-Prieta earthquake, J. Geophys. Res., v.105, 5,615-5,634, 2000.

Shen ZK, Jackson DD, Feng Y, Cline M, Kim M, Fang P, Bock Y. 1994. Postseismic deformation following the Landers earthquake, California, 28 June 1992, *Bull. Seis. Soc. Am.* 84:780-791

Shen, Z. K., D. D. Jackson and B. Ge, Crustal Deformation Across and Beyond the Los Angeles Basin from Geodetic Measurements, Journal of Geophysical Research, 101, no. 27, pp. 957-27, 980, 1996.

Tsuji, H., Y. Hatanaka, T. Sagiya, and M. Hashimoto, Coseismic crustal deformation from the 1994 Hokkaido-Toho-Oki earthquake monitored by a nationwide continuous GPS array in Japan, Geophysical Res. Letters *22,* 1669-1672, 1995.

Wernicke, Brian; Friedrich, Anke M.; Niemi, Nathan A., and others, Dynamics of plate boundary fault systems from Basin and Range Geodetic Network (BARGEN) and geological data GSA Today 10, no. 11 (200011): 1-7 , 2000.

Wicks, C., W. Thatcher, and D. Dzurisin, Migration of fluids beneath Yellowstone Caldera inferred from satellite radar interferometry, Science, vol.282, no.5388, pp.458-462, 1998.

Wright, T., B. Parsons, and E. Fielding, Measurement of interseismic strain accumulation across the North Anatolian Fault by satellite radar interferometry, Geophysical Research Letters, vol.28, no.10, pp.2117-2120, 2001.

Wyatt, F. K., Displacement of surface monuments; vertical motion, *J. Geophys. Res.*, v. 94, p. 1655-1664, 1989.

Zhang, J., Y. Bock, H. Johnson, P. Fang, S. Williams, J. Genrich, S. Wdowinski, and J. Behr, Southern California permanent GPS geodetic array: Error analysis of daily position estimates and site velocities, *J. Geophys. Res.* *102,* 18,035-18,055, 1997.

4 Management Plan

This is an ambitious effort, involving both technique and code development, and analysis of two large and complex data sets. To accomplish these goals we have developed a cost-effective management plan, taking advantage of existing funding, as well as significant contributions from independently funded collaborators.

P. Segall will serve as Principal Investigator for the project and is responsible for its organization and overall progress. He will oversee the code development for the distributable form of the NIF, and will work with Co-Investigator McGuire on the development of the Network Strain Filter. He will also supervise the graduate student in developing both steady-state and temporally varying models of the SCIGN data. Finally, he will coordinate with McGuire and Japanese colleagues on the analysis of the Tokai data. Co-Investigator McGuire will have primary responsibility for analysis of the Japanese data and development of the Network Strain Filter. Co-Investigator Hurst will coordinate the development of the geometric fault model for southern California and will be responsible for characterizing the errors in the GPS data. Specifically, he will Interface NIF with SCIGN analysis (1 month/yr). Integrate the NIF into the GEM environment (2 wks first year). Provide fault database(s) to NIF (1 wk first year, and 2nd year).

The Postdoctoral Fellow will be responsible for actually producing distributable code for the Network Inversion Filter. He/she will also develop methods for including alternate data types in the NIF, including InSAR. Finally, he/she will work with the graduate student on modeling the SCIGN data. The graduate student will focus on developing fault models for southern California and analyzing the SCIGN data.

We have developed collaborative relations with Japanese scientists working on GPS and SAR. These collaborators add tremendous breadth to our efforts at no cost. In addition, they bring access to important GPS and other data. Dr. Shinichi Miyazaki (E.R.I, U. Tokyo) will be spending two years at Stanford, beginning in 2003. Prof. T. Kato (E.R.I, U. Tokyo) and Drs. T. Sagiya (G.S.I.) and Y. Hatanaka have agreed to collaborate on the study of the Tokai GPS data.

There are a number of ongoing and planned studies at Stanford that will add to the proposed work without cost to this project. We anticipate funding the remainder of the postdoc's effort with pre-Earthscope funds directed at network design for the proposed Plate Boundary Observatory. Part of this work will be to develop the needed error models to include strain data into the NIF. Furthermore, we have ongoing studies to utilize the NIF to study space time evolution of fault slip on the Parkfield segment of the San Andreas fault, as well as fault slip and rift-zone spreading on Kilauea volcano. The volcano is rapidly deforming and experiences frequent episodes of transient deformation. Kilauea also presents significant volcanic, seismic, and tsunami hazards. An extensive GPS network has been in place for several years.

5 Cost Plan

6 Current and Pending Research

7 Resumes